TITLE:

Investigations on the Stress in Circular Shaft Linings

AUTHOR(S):

HIRAMATSU, Yoshio; OKA, Yukitoshi; OGINO, Shōji

Investigations on the Stress in Circular Shaft Linings

By

Yoshio HIRAMATSU*, Yukitoshi OKA* and Shōji OGINO**

For the purpose of contributing data for the reasonable design of shaft linings, the authors have tried, at first, to measure the stress in the linings of several vertical shafts recently sunk in coal mines by means of a photoelastic stressmeter, and have obtained data for estimating the earth pressure that may act on shaft linings when they are sunk into ground of various conditions.

Secondly the stresses in a circular shaft lining caused by various states of earth pressure are analysed by the theory of elasticity, and the stress concentration due to irregular earth pressure is clarified. Part I describes the results of the stress measurements, and Part II the results of the analysis.

Part I. Measurement of Stress in Shaft Linings

1. Introduction

In coal mines of our country, large shafts have been excavated in circular shape and lined firmly with concrete. At present, however, little is known about the earth pressure acting on such shaft linings, so that their design depends upon experience or upon empirical formulas, which frequently give different thicknesses for the linings.

As it is believed that a theoretical evaluation of the earth pressure acting on shaft linings is difficult, the authors have attempted to measure the stress in the linings of shafts recently sunk into ground of various conditions.

2. Method of stress measurement

In order to measure the stress in shaft linings, a photoelastic stressmeter and glass test pieces devised by the authors have been employed. This means of stress measurement has the advantage of allowing measurements over a long period of time with constant accuracy. When a lining is built, photoelastic test pieces are set tightly into small cavities on the inner surface of the lining with hard adhesive. At this moment the earth pressure, and consequently the stress

* Department of Mining
** Faculty of Engineering, Yamaguchi University

in the lining, is doubtless zero. If, afterwards, the lining is subjected to earth pressure, the stress on the inner surface of the lining increases. The stress in the test pieces will vary with the variation in the stress on the inner surface of the lining. By measuring the stress in the test piece with a photoelastic stress-meter, the stress on the inner surface of the lining is determined.

The test pieces are short cylinders of borosilicate glass, either hollow or
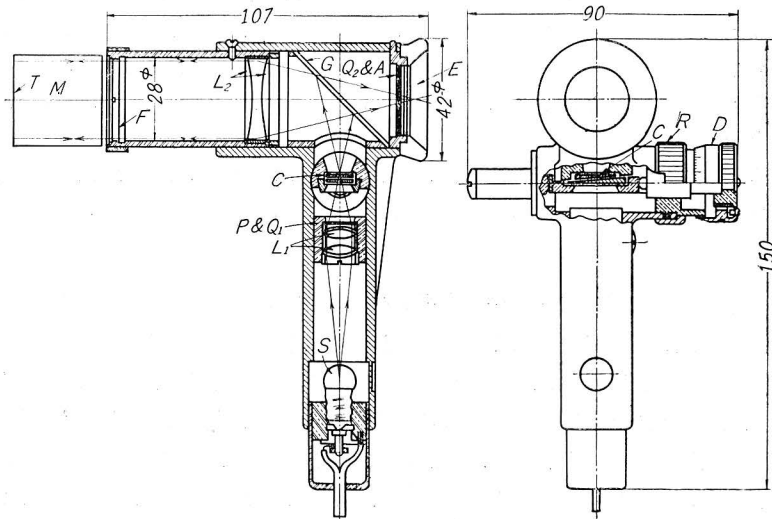
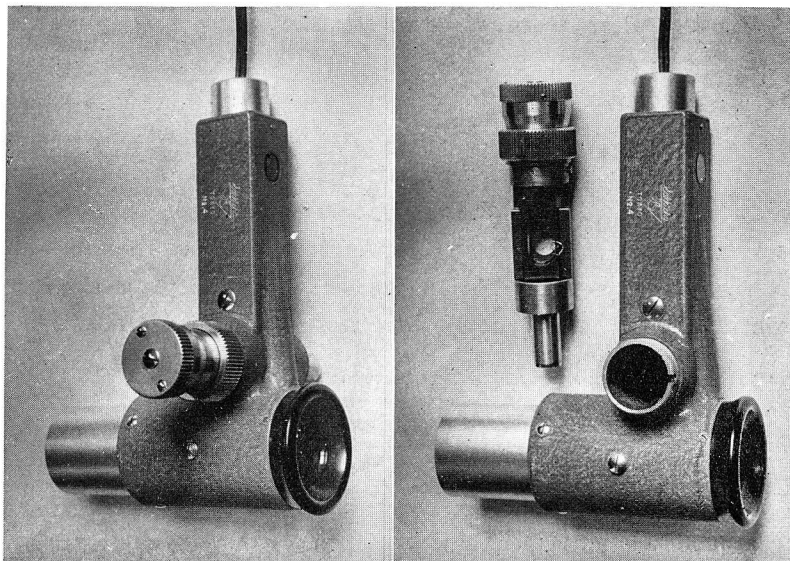Fig. 1(a). Construction of the photoelastic stressmeter.

Fig. 1(b). Aspects of the photoelastic stressmeter.

solid, 35 mm in diameter, 30 mm long. The inner diameter of the hollow test piece is 5 mm. In the early days of measurement, only the hollow cylindrical test pices were used and the stress pattern was observed with a portable photo-elastic apparatus of the original type that had no compensator. The stress in the lining was determined from the observation of the stress pattern in the glass test piece.

Recently the apparatus was improved by attaching a compensator, and the stress is now determined more quantitatively. Fig. 1 (a) and (b) show the construction and the aspect of the improved apparatus. Concerning the details of the original apparatus and how to use it, the reader is referred to other papers already published[2].

The effect of creep in the concrete on the stress pattern or on the reading of the compensator was not considered, but it is supposed that this effect is very small.

3. Results of stress measurement

(a) At the Hatsushima Exhaust Shaft of the Miike Coal Mine

The Hatsushima Exhaust Shaft of the Miike Coal Mine, Mitsui Mine Co., was sunk at the center of the artificial island named "Hatsushima" which was built in the Ariake Sea for that purpose. The upper part of this shaft, down to 120 m in depth, of 9.6 m and 7.0 m outer and inner diameter, was sunk by the sinking well method through quarternary strata. Four test pieces were set on the inner surface of the shaft well at depths of 22 m, 62.6 m and 82.6 m. At each depth, the four test pieces were placed at equal intervals, namely on the north, south, east and west sides of the inner surface of the well. The setting of test pieces was practised at the top of the well just after it was extended, from Nov. 1952 to May 1953. In January 1954, when the sinking of the well and the cementation of the space behind the shaft well had been completed, the stress measurements were carried out with the original type of the photoelastic apparatus.

The test pieces at the depth of 22 m showed only a low stress that was difficult to measure. It was found that the stress on the inner surface of the well is horizontal. The magnitude of the stress is as shown in Table 1.

Table 1. The results of stress measurement at the Hatsushima Shaft.

Depth (m)	Horizontal tangential stress (kg/cm^2)				
	North	South	East	West	Average
62.6	27	*	26	18	23.7
82.6	28	30	28	29	28.8

* The datum was missed.

If the shaft well were subjected to an earth pressure equal to the hydrostatic pressure, the horizontal tangential stress on the inner surface of the well would be 26.7, and 35.2 kg/cm² at the depths of 62.6 m and 82.6 m respectively according to the theory of the strength of material. It is seen, therefore, that the earth pressure is somewhat lower than the hydrostatic pressure in the quarternary strata under the Ariake Sea.

(b) At the Ikari Shaft of the Tagawa Coal Mine

The Ikari Shaft of the Tagawa Coal Mine, Mitsui Mine Co., 660 m deep, was excavated in rather good ground, and lined firmly with concrete. It was thought, therefore, that little trouble would arise concerning earth pressure. Around the lower part of the shaft bottom, however, there appeared a weak shale stratum, causing some fear that the lower part of the shaft bottom lining might be subjected to increasing earth pressure.

In order to study it, twenty test pieces were set on the inner surface of the shaft bottom lining, and the variation in stress was observed over a long period of time with a photoelastic stressmeter of the original type. Fig. 2 shows a
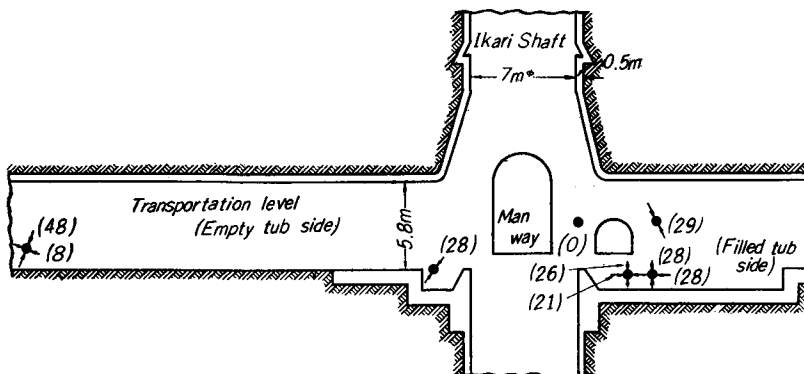

Fig. 2. Results of measurements at the bottom of the Ikari Shaft. Small circles show the position of the test pieces, and arrows accompanied by numerals represent the direction and magnitude in kg/cm² of the principal stresses.

vertical section through the center line of the transportation level, viewed toward the dip side. The strike is parallel to the center line of the level. The dip angle is 15°. The lining was constructed in the following way. At first the excavated space was supported with rail rings and steel bars crossing them. For the lower part of the space where the weak shale appeared, the steel bars were replaced with rails. This steel construction was covered with a concrete lining, 50 cm thick at the upper part, and 1 m thick at the lower part.

The test pieces were set during the period from 28 Aug. to 23 Oct. 1954. The observation of the stress pattern in the test pieces showed that the stress at first increased a little with time but became constant before long. After that state was reached, observations were discontinued.

However observations were again attempted in Nov. 1959, namely more than five years after the lining was built. Then it was found that the silvered bottom surfaces on the great majority of the test pieces were so corroded that observation of the stress pattern was impossible. (Recently such a failure has been eliminated by employing "Araldite Cold Setting Adhesive, Type 121" in place of cement mortar, as the adhesive.) Therefore, observations were carried out with those test pieces that were in good condition. Those results are shown in Fig. 2, the stress on the inner surface of the bottom of the Ikari Shaft varying from 0 to 50 kg/cm² according to the condition of the ground behind the lining.

(c) At the Exhaust Shaft of the Ooyūbari Coal Mine

The Exhaust Shaft, 6 m in diameter, of the Ooyūbari Coal Mine, Mitsubishi Mining Co., meets a circular tunnel of the same diameter at the bottom, 760 m deep. The ground around the shaft bottom consists of weak "Horokabetsu Shale". Experience has shown that in this shale no tunnel is easy to support. Table 2 shows the strength of this shale.

Table 2. Strength of Horokabetsu Shale

Direction of loading to the stratification	Compression		Tension	
	No. of test pieces	Strength (kg/cm²)	No. of test pieces	Strength (kg/cm²)
Normal	3	390	3	24
Parallel	2	486	2	30

Under these circumstances, field tests of the earth pressure on a model shaft lining were conducted in the following way. The experimental shaft bottom space, 1/2 in scale, was excavated beforehand just at the position where the true shaft bottom was to be. It was lined with concrete rigidly, 20 cm thick and many test pieces were set on the inner surface. The variation in stress was measured for 170 days from the day on which the test pieces were set (28 May 1954) with a photoelastic stressmeter of the original type. Fig. 3 shows the shape of the experimental shaft bottom, the position of the test pieces and the direction of the stress measured. Fig. 4 illustrates the variation in the greater principal stress with time. From this measurement it was found that the earth pressure increased gradually with time to reach 5~30 kg/cm² and was still increasing even after 170 days from the time of construction of the lining, except
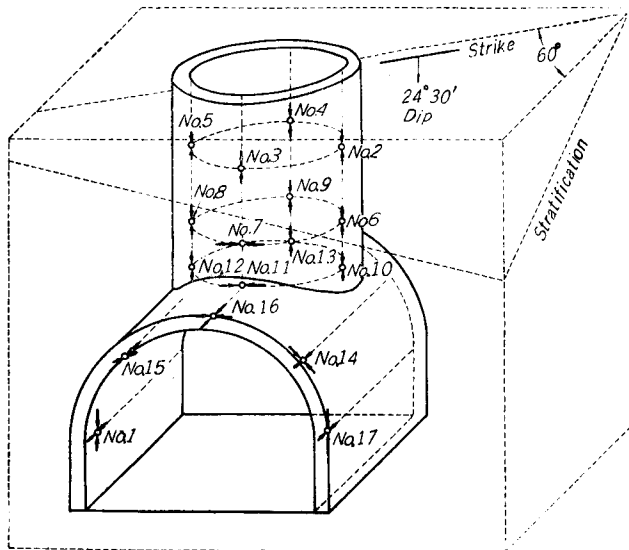
Fig. 3.   Position of test pieces and direction of principal stresses
measured on the lining of the model shaft bottom.

for Test Piece No. 11.   It was
supposed, however, that the
earth pressure would not in-
crease so much thereafter.

Test piece No. 11 showed
unusual variation in stress.
The reason seems to be that
the roof rock near the junction
of the shaft and the tunnel is
apt to fall early and press
the lining, and that once the
loose rock pieces slip, the
stress in the lining may vary

Fig. 4.   Variation in the greater principal stresses with
time in the lining of the model shaft bottom.

suddenly.   The authors have found by barodynamic experiments that such a
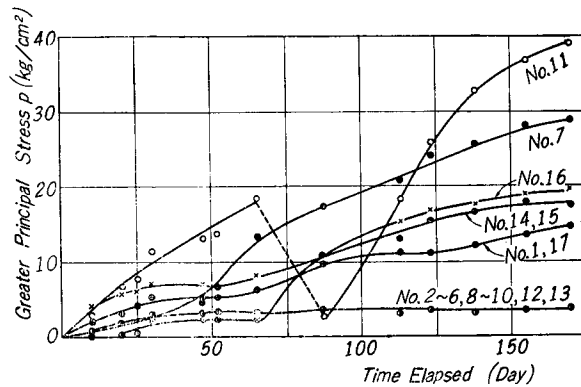portion of roof rock is most inclined to fall, but that this failure of rock ceased
before long[3].

(d)   At the Central Shaft of the Ponbetsu Coal Mine

The Central Shaft of the Ponbetsu Coal Mine, Sumitomo Coal Mining Co.,
was sunk in Neogene ground consisting of so-called Horonai shale.   This shale
is not only weak, but is also so disturbed by two large faults running near by

that we can hardly find the stratification in the ground. Fig. 5 shows the relative positions of the shaft, the coal seams and the faults. As it is very interesting to clarify the earth pressure acting on the lining of a shaft sunk into such bad ground, we have measured the stress in the shaft lining with the improved photoelastic stressmeter.

Fig. 5. Relative position of the Ponbetsu shaft to coal seams and faults.

The shaft was lined with two layers of concrete blocks, namely with an outer layer of weak hollow blocks and an inner layer of strong solid blocks. A cement mortar layer between the two layers, about 1 cm thick, prevents water from penetrating. The space between the ground and the outer layer was also packed with cement mortar. Fig. 6 shows the two kinds of blocks and the construction of the lining.

The solid blocks were produced with strong concrete, about 400 kg/cm² in compressive strength, the ratio of cement, sand and gravel being 1 : 2 : 4, while the hollow blocks were produced with weak and soft concrete, of one part cement and seven parts burnt rubbish. The strength of the hollow block is not definite, but it seems to be about 50 kg/cm²,
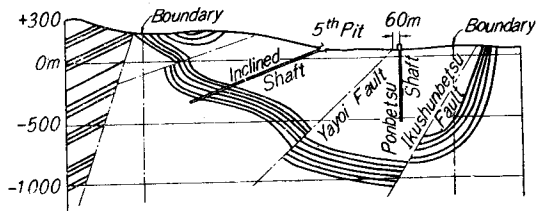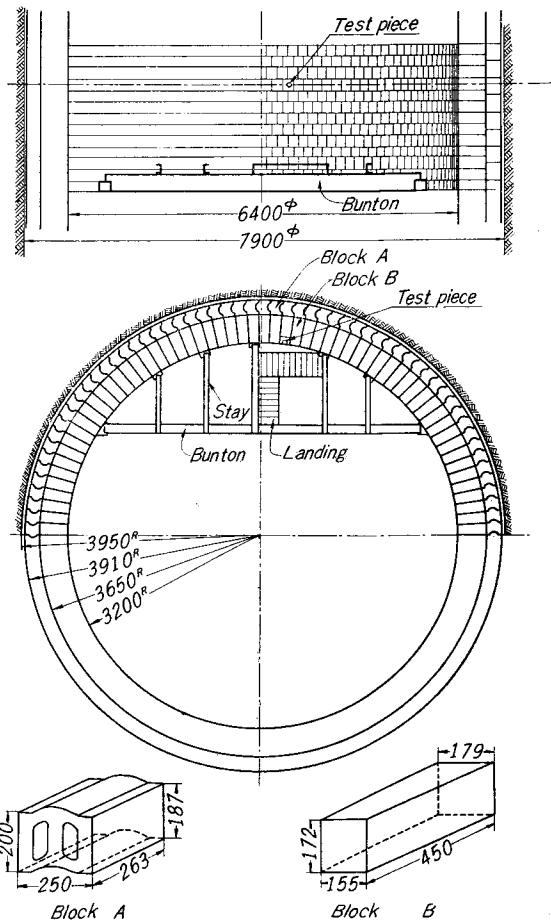

Fig. 6. Shape of concrete blocks and construction of the lining of the Ponbetsu Shaft.

In any case, the lining of the Ponbetsu Shaft is regarded as a rigid construction so long as no break occurs, but once the hollow blocks break, they act as yielding packing for the inner layer.

The glass test pieces were spaced every 9.83 m, one at each place, in a vertical line on the inner surface of the lining. Hollow cylindrical test pieces were used down to a depth of 79 m, but because the earth pressure was so strong that they were soon crushed, solid cylindrical test pieces were adopted for the lower part. The depth of the shaft is 550 m, but the measurements were carried out only down to a depth of 275.7 m. We are intending, however, to carry out the measurement for the lower part of the shaft lining after the shaft is completed.

The depth at which each test piece is set and the results of measurement are shown in Fig. 7. From this figure we can see that the stress in the lining, and consequently the earth pressure acting on the lining, is related not to the depth but to the condition of the ground, and that the stress increases at first and fluctuates afterwards with time. Fortunately, it is noticed, however, that the stress in any test piece shows a tendency to decrease slightly about a year or so after excavation.
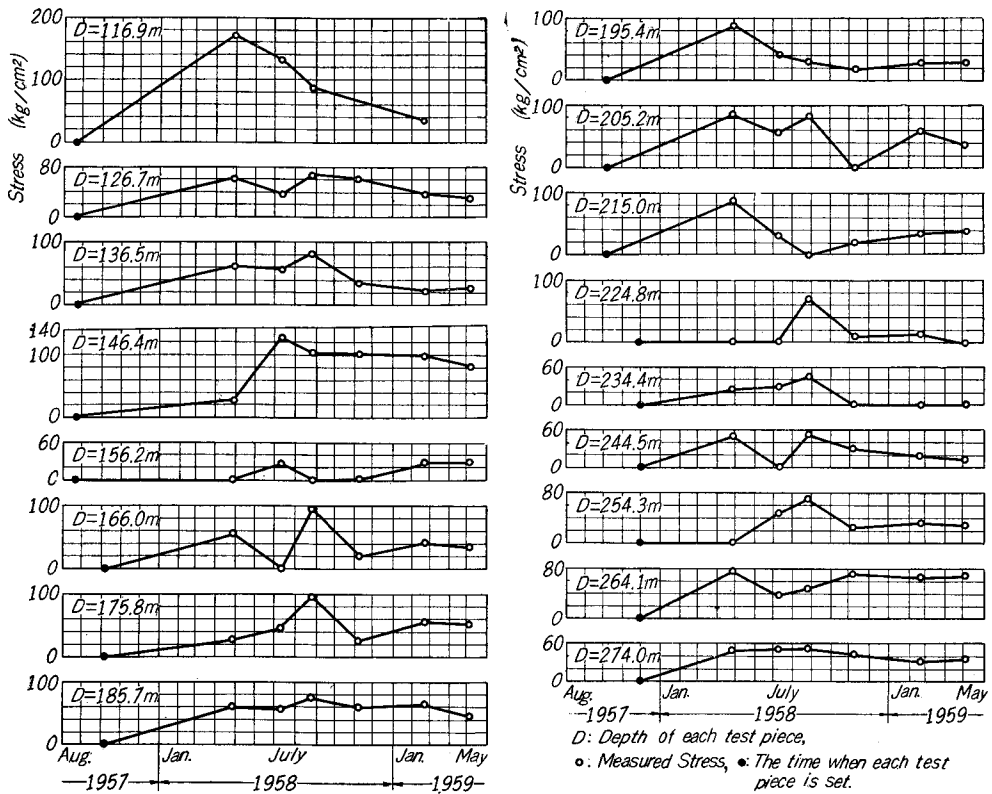
Fig. 7. Results of stress measurements in the Ponbetsu Shaft.

4. Conclusion

Though the accuracy of this stress measurement was not satisfactory in the early days of this measurement, the following information has been obtained concerning the stress in rigid shaft linings. In solid ground, even though it is not strong, the stress in a shaft lining remains almost zero or tends to a low value, say 30 kg/cm², i.e. a lining is subjected at most to a very small earth pressure that may be due to the creep of rock. In loose or crushed ground, however, shaft linings are subjected to an earth pressure that frequently causes high stresses in the linings, the magnitude of which depends upon the condition of the ground. It is essential, for reasonable design of shaft linings, to estimate the earth pressure, and it is believed that the results described above will be of service in making this estimation.

Part II. Theoretical Studies on the Stress in a Shaft Lining Caused by Earth Pressure

1. Introduction

As it has been found, in Part I, that in loose or crushed ground, shaft linings are subjected to increasing earth pressure that may cause high stresses in the linings that are not to be disregarded, in Part II an analysis of stress in shaft linings caused by several states of earth pressure is given.

2. Analysis

(a) Stress in a circular shaft lining subjected to a number of intermittent earth pressures

Let the inner and outer radii of a circular shaft lining be a and b cm respectively, and assume the intermittent earth pressures p_1, p_2, $\cdots$, p_m kg/cm² act on small sections of the outer surface as shown in Fig. 8, where m designates the number of the earth pressures. The center angles of those small sections are denoted as $2\phi_1$, $2\phi_2$, $\cdots$, $2\phi_m$, and the angles between the initial line of the polar coordinates and the radii passing through the centers of those sections as θ_1, θ_2, $\cdots$, θ_m. In the following
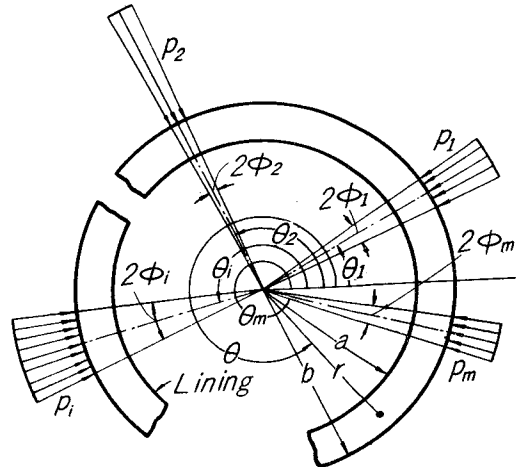

Fig. 8.

analysis, let us assume that the earth pressures acting on a portion of the lining cut by any two horizontal sections are in equilibrium, namely that

$$\left.\begin{array}{l} \sum_{i=1}^{m} p_i \sin \phi_i \cos \theta_i = 0 , \\[2mm] \sum_{i=1}^{m} p_i \sin \phi_i \sin \theta_i = 0 . \end{array}\right\} \qquad\qquad\cdots\cdots\cdots\cdots\cdots(1)$$

Now, the general formula of Airy's stress function $\varPhi$ in polar coordinates is as follows:

$$\begin{aligned} \varPhi =\; & A_0 r^2 + B_0 \log r + D_0 \log r + K_0 r^2 \theta + H_0 \theta \\ & + A_1 r^3 \cos \theta + B_1 r^{-1} \cos \theta + C_1 r \theta \sin \theta + D_1 r \log r \cos \theta \\ & + A_1' r^3 \sin \theta + B_1' r^{-1} \sin \theta - C_1' r \theta \cos \theta + D_1' r \log r \sin \theta \\ & + \sum_{n=2}^{\infty} \{(A_n r^{n+2} + B_n r^{-n} + C_n r^n + D_n r^{-n+2}) \cos n\theta \\ & + \sum_{n=2}^{\infty} (A_n' r^{n+2} + B_n' r^{-n} + C_n' r^n + D_n' r^{-n+2}) \sin n\theta \} , \qquad \cdots\cdots\cdots\cdots\cdots(2) \end{aligned}$$

where A_0, B_0, D_0, K_0, H_0, A_1, B_1, $\cdots$ are constants. Since it is required that any displacement must single-valued, the equation of displacement which is derived from Eq. 2 must have no term that is not single-valued. Therefore,

$$D_0 = K_0 = 0 .$$

Consequently each stress, σ_r, σ_θ, and $\tau_{r\theta}$ is given by:

$$\begin{aligned} \sigma_r =\; & 2A_0 + B_0 r^{-2} \\ & + 2\{A_1 r - B_1 r^{-3} + (2C_1 + D_1) r^{-1}\} \cos \theta \\ & + 2\{A_1' r - B_1' r^{-3} + (2C_1' + D_1') r^{-1}\} \sin \theta \\ & - \sum_{n=2}^{\infty} [\{(n-2)(n+1)A_n r^n + n(n+1)B_n r^{-n-2} \\ & \qquad\qquad + n(n-1)C_n r^{n-2} + (n+2)(n-1)D_n r^{-n}\} \cos n\theta \\ & \qquad - \{(n-2)(n+1)A_n' r^n + n(n+1)B_n' r^{-n-2} \\ & \qquad\qquad + n(n-1)C_n' r^{n-2} + (n+2)(n-1)D_n' r^{-n}\} \sin n\theta] , \qquad \cdots\cdots(3a) \end{aligned}$$

$$\begin{aligned} \sigma_\theta =\; & 2A_0 - B_0 r^{-2} \\ & + 2(3A_1 r + B_1 r^{-3} + D_1 r^{-1}) \cos \theta \\ & + 2(3A_1' r + B_1' r^{-3} + D_1' r^{-1}) \sin \theta \\ & + \sum_{n=2}^{\infty} [\{(n+2)(n+1)A_n r^n + n(n+1)B_n r^{-n-2} \\ & \qquad\qquad + n(n-1)C_n r^{n-2} + (n-2)(n-1)D_n r^{-n}\} \cos n\theta \\ & \qquad + \{(n+2)(n+1)A_n' r^n + n(n+1)B_n' r^{-n-2} \\ & \qquad\qquad + n(n-1)C_n' r^{n-2} + (n-2)(n-1)D_n' r^{-n}\} \sin n\theta] , \qquad \cdots\cdots(3b) \end{aligned}$$

$$\tau_{r\theta} = H_0 r^{-2}$$
$$+2(A_1 r - B_1 r^{-3} + D_1 r^{-1}) \sin\theta$$
$$-2(A_1' r - B_1' r^{-3} + D_1' r^{-1}) \cos\theta$$
$$+\sum_{n=2}^{\infty} [n\{(n+1)A_n r^n - (n+1)B_n r^{-n-2}$$
$$+(n-1)C_n r^{n-2} - (n-1)D_n r^{-n}\} \sin n\theta$$
$$-n\{(n+1)A_n' r^n - (n+1)B_n' r^{-n-2}$$
$$+(n-1)C_n' r^{n-2} - (n-1)D_n' r^{-n}\} \cos n\theta] . \qquad \cdots\cdots\cdots(3c)$$

As for boundary conditions at the inner surface,

$$(\sigma_r)_{r=a} = 0 , \quad (\tau_{r\theta})_{r=a} = 0 , \qquad \cdots\cdots\cdots\cdots\cdots(4a)$$

and at the outer surface,

$$\left.\begin{array}{ll} (\sigma_r)_{r=b} = p_i , & \text{for} \quad \theta_i - \phi_i \leqq \theta \leqq \theta_i + \phi_i , \\ (\sigma_r)_{r=b} = 0 , & \text{for} \quad \theta_i + \phi_i < \theta < \theta_{i+1} - \phi_{i+1} . \end{array}\right\} \quad \cdots\cdots\cdots\cdots(4b)$$

$$(\tau_{r\theta})_{r=b} = 0 , \qquad \cdots\cdots\cdots\cdots(4c)$$

where $i = 1, 2, \cdots, m$.

Developing Eq. (4b) into a Fourier series, we obtain

$$(\sigma_r)_{r=b} = a_0 + a_1 \cos\theta + b_1 \sin\theta + \sum_{n=2}^{\infty} (a_n \cos n\theta + b_n \sin n\theta) , \qquad \cdots\cdots\cdots(5)$$

where

$$a_0 = \frac{1}{2\pi}\int_0^{2\pi} (\sigma_r)_{r=b} d\theta , \qquad a_1 = \frac{1}{\pi}\int_0^{2\pi} (\sigma_r)_{r=b} \cos\theta d\theta ,$$

$$a_n = \frac{1}{\pi}\int_0^{2\pi} (\sigma_r)_{r=b} \cos n\theta d\theta , \quad b_1 = \frac{1}{\pi}\int_0^{2\pi} (\sigma_r)_{r=b} \sin\theta d\theta ,$$

$$b_n = \frac{1}{\pi}\int_0^{2\pi} (\sigma_r)_{r=b} \sin n\theta d\theta .$$

Consequently, Eq. (4b) is rewritten as:

$$(\sigma_r)_{r=b} = \frac{2}{\pi}\sum_{i=1}^{m} p_i\left\{\frac{\phi_i}{2} + \sum_{n=2}^{\infty} \frac{1}{n} \sin n\phi_i \ (\cos n\theta_i \cos n\theta + \sin n\theta_i \sin n\theta)\right\} . \qquad \cdots\cdots(6)$$

From these boundary conditions, the constants in Eq. (3) are determined as follows:

$$\left.\begin{array}{l} A_0 = \dfrac{1}{2\pi}\sum_{i=1}^{m} p_i\phi_i\left(\dfrac{b}{a}\right)^2 , \quad B_0 = -\dfrac{1}{\pi}\sum_{i=1}^{m} p_i\phi_i\dfrac{b^2 a^2}{b^2 - a^2} , \\ H_0 = 0 , \\ A_1 = B_1 = C_1 = D_1 = A_1' = B_1' = C_1' = D_1' = 0 , \\ A_n = \dfrac{\beta}{\alpha}\dfrac{1}{n+1}\dfrac{b^n}{a^{2n}}\left\{\left(\dfrac{b}{a}\right)^{2n} + n\left(\dfrac{b}{a}\right)^2 - (n+1)\right\} , \end{array}\right.$$

$$B_n = -\frac{\beta}{\alpha}\frac{1}{n+1}b^{n+2}\left\{(n+1)\left(\frac{b}{a}\right)^{2n}-n\left(\frac{b}{a}\right)^{2n-1}-1\right\},$$

$$C_n = -\frac{\beta}{\alpha}\frac{1}{n-1}\frac{b^n}{a^{2n-2}}\left\{\left(\frac{b}{a}\right)^{2n+2}+(n-1)\left(\frac{b}{a}\right)^2-n\right\},$$

$$D_n = \frac{\beta}{\alpha}\frac{1}{n-1}b^n\left\{n\left(\frac{b}{a}\right)^{2n+2}-(n-1)\left(\frac{b}{a}\right)^{2n}-1\right\},$$

$$A_n' = \frac{\gamma}{a}\frac{1}{n+1}\frac{b^n}{a^{2n}}\left\{\left(\frac{b}{a}\right)^{2n}+n\left(\frac{b}{a}\right)^2-(n+1)\right\},$$

$$B_n' = -\frac{\gamma}{a}\frac{1}{n+1}b^{n+2}\left\{(n+1)\left(\frac{b}{a}\right)^{2n}-n\left(\frac{b}{a}\right)^{2n-2}-1\right\},$$

$$C_n' = -\frac{\gamma}{\alpha}\frac{1}{n-1}\frac{b^n}{a^{2n-2}}\left\{\left(\frac{b}{a}\right)^{2n+2}+(n-1)\left(\frac{b}{a}\right)^2-n\right\},$$

$$D_n' = \frac{\gamma}{a}\frac{1}{n-1}b^n\left\{n\left(\frac{b}{a}\right)^{2n+2}-(n-1)\left(\frac{b}{a}\right)^{2n}-1\right\},$$

$$\cdots\cdots\cdots\cdots(7)$$

where

$$\alpha = \left\{\left(\frac{b}{a}\right)^{2n}-1\right\}^2-\left\{\left(\frac{b}{a}\right)^2-1\right\}^2 n^2\left(\frac{b}{a}\right)^{2n-2},$$

$$\beta = \frac{1}{n\pi}\sum_{i=1}^{m}p_i\sin n\phi_i\cos n\theta_i,$$

$$\gamma = \frac{1}{n\pi}\sum_{i=1}^{m}p_i\sin n\phi_i\sin n\theta_i.$$

$$\cdots\cdots\cdots\cdots(8)$$

By substituting the constants in Eqs. (3a), (3b) and (3c) with Eq. (7), each stress σ_r, σ_θ and $\tau_{r\theta}$ is obtained. These equations will be omitted here because they are very long, and only the tangential stresses on the inner and outer surfaces will be given below.

$$(\sigma_\theta)_{r=a} = \frac{2}{\pi}\sum_{i=1}^{m}p_i\phi_i\frac{b^2}{b^2-a^2}-\frac{4}{\pi}\frac{b^2-a^2}{a^2}\sum_{n=2}^{\infty}\left[\frac{1}{\alpha}\left(\frac{b}{a}\right)^n\left\{\left(\frac{b}{a}\right)^{2n}-1\right\}\right.$$

$$\left.\times\sum_{i=1}^{m}p_i\sin n\phi_i\cos n(\theta_i-\theta)\right],$$

$$(\sigma_\theta)_{r=a} = \frac{1}{\pi}\sum_{i=1}^{m}p_i\phi_i\frac{b^2+a^2}{b^2-a^2}+\frac{2}{\pi}\sum_{n=2}^{\infty}\left[\frac{1}{n\alpha}\left\{\left(\frac{b^{2n}}{a^{2n}}-1\right)^2\right.\right.$$

$$\left.\left.+\left(\frac{b^2-a^2}{a^2}\right)^2 n^2\left(\frac{b}{a}\right)^{2n-2}\sum_{i=1}^{m}p_i\sin n\phi_i\cos n(\theta_i-\theta)\right\}\right].$$

$$\cdots\cdots\cdots(9)$$

(b) Stress in a circular shaft lining subjected to an earth pressure distributed elliptically

(i) When the distribution of earth pressure acting on a circular shaft lining is represented by $p\cos^2\theta$, as shown in Fig. 9 (2), the boundary condition in Eq. (4b) is replaced by

$$(\sigma_r)_{r=b} = p\cos^2\theta.$$
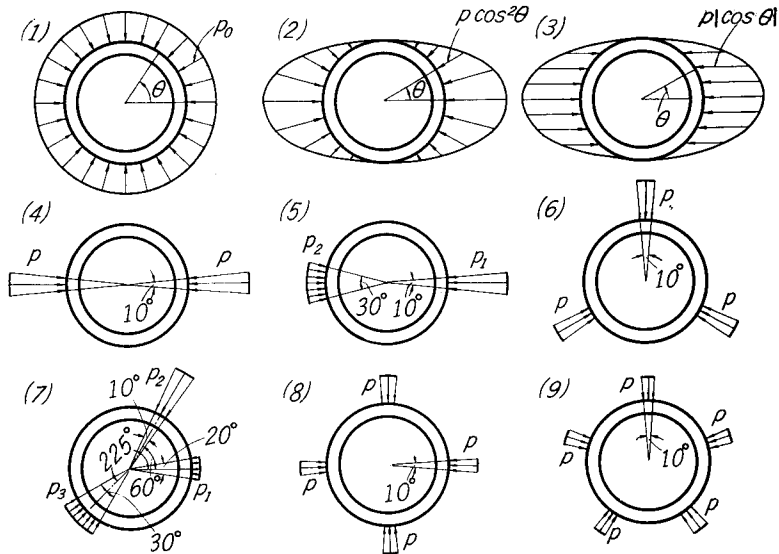
$$\cdots\cdots\cdots\cdots(10)$$

Fig. 9. Nine states of earth pressure distribution on a circular shaft lining.

Accordingly, the constants in Eqs. (3a), (3b) and (3c) are determined as follows:

$$
\left.
\begin{aligned}
&A_0 = \frac{p}{4}\frac{b^2}{b^2-a^2}, \qquad B_0 = -\frac{p}{2}\frac{b^2a^2}{b^2-a^2}, \\
&A_2 = \frac{p}{12}\frac{b^2}{(b^2-a^2)^3}(b^2+3a^2), \\
&B_2 = -\frac{p}{12}\frac{b^4a^4}{(b^2-a^2)^3}(3b^2+a^2), \\
&C_2 = -\frac{p}{4}\frac{b^2}{(b^2-a^2)^3}(b^4+b^2a^2+2a^4), \\
&D_2 = \frac{p}{4}\frac{b^2a^2}{(b^2-a^2)^3}(2b^4+b^2a^2+a^4),
\end{aligned}
\right\}
\quad \cdots\cdots\cdots\cdots\cdots(11)
$$

All the other constants$=0$.

Consequently, each stress is obtained as shown below.

$$
\left.
\begin{aligned}
\sigma_r &= \frac{1}{2}\frac{b^2}{b^2-a^2}\Big[(1-a^2r^{-2})+\frac{1}{(b^2-a^2)^2}\{b^4+b^2a^2+2a^4 \\
&\quad -2a^2(2b^4+b^2a^2+a^4)r^{-2}+b^2a^4(3b^2+a^2)r^{-4}\}\cos 2\theta\Big]p, \\
\sigma_\theta &= \frac{1}{2}\frac{b^2}{b^2-a^2}\Big[(1+a^2r^{-2})+\frac{1}{(b^2-a^2)^2}\{2(b^2+3a^2)r^2 \\
&\quad -(b^4+b^2a^2+2a^4)-b^2a^4(3b^2+a^2)r^{-4}\}\cos 2\theta\Big]p, \\
\tau_{r\theta} &= \frac{1}{2}\frac{b^2}{(b^2-a^2)^3}\{(b^2+3a^2)r^2-(b^4+b^2a^2+2a^4) \\
&\quad -a^2(2b^4+b^2a^2+a^4)r^{-2}+b^2a^4(3b^2+a^2)r^{-4}\}(\sin 2\theta)p.
\end{aligned}
\right\}
\quad \cdots\cdots(12a)
$$

The tangential stresses on the inner and outer surfaces are:

$$(\sigma_\theta)_{r=a} = \left\{ \frac{b^2}{b^2-a^2} - \frac{2b^2(b^2+a^2)}{(b^2-a^2)^2} \cos 2\theta \right\} p \, ,$$

$$(\sigma_\theta)_{r=b} = \frac{1}{2} \left\{ \frac{b^2+a^2}{b^2-a^2} + \frac{b^4-6b^2a^2+a^4}{(b^2-a^2)^2} \cos 2\theta \right\} p \, .$$

$$\cdots\cdots\cdots\cdots(12b)$$

(ii) When the distribution of the earth pressure acting on a lining is represented by $p|\cos\theta|$, as shown in Fig. 9 (3), Eqs. (4b) and (4c) are replaced by

$$(\sigma_r)_{r=b} = p \cos^2 \theta \, ,$$

$$(\tau_{r\theta})_{r=b} = p \cos \theta \sin \theta \, .$$

$$\cdots\cdots\cdots\cdots(13)$$

Accordingly, the constants in Eqs. (3a), (3b) and (3c) are determined as follows:

$$A_0 = \frac{p}{4} \frac{b^2}{b^2-a^2} \, , \qquad B_0 = -\frac{p}{2} \frac{b^2a^2}{b^2-a^2}$$

$$A_2 = \frac{p}{6} \frac{b^4}{(b^2-a^2)^3} \, , \qquad B_2 = -\frac{p}{12} \frac{b^4a^4}{(b^2-a^2)^3}(3b^2-a^2)$$

$$C_2 = -\frac{p}{4} \frac{b^4}{(b^2-a^2)^3}(b^2+a^2) \, , \quad D_2 = \frac{p}{2} \frac{b^6a^2}{(b^2-a^2)^3} \, ,$$

$$\text{All the other constants} = 0 \, .$$

$$\cdots\cdots\cdots\cdots(14)$$

The tangential stresses on the inner and outer surfaces are:

$$(\sigma_\theta)_{r=a} = \left\{ \frac{b^2}{b^2-a^2} - \frac{2b^4}{(b^2-a^2)^2} \cos 2\theta \right\} p \, ,$$

$$(\sigma_\theta)_{r=b} = \frac{1}{2} \left\{ \frac{b^2+a^2}{b^2-a^2} + \frac{(b^2+a^2)(3b^2-a^2)}{a^2(b^2-a^2)} \cos 2\theta \right\} p \, .$$

$$\cdots\cdots\cdots\cdots(15)$$

(iii) When a uniform earth pressure acts on a lining, as shown in Fig. 9 (1), Equation (4b) is replaced by

$$(\sigma_r)_{r=b} = p \, ,$$

$$\cdots\cdots\cdots\cdots(16)$$

and the constants are determined as follows:

$$A_0 = \frac{1}{2} \frac{b^2}{b^2-a^2} p \, , \quad B_0 = -\frac{b^2a^2}{b^2-a^2} p \, ,$$

$$\text{All the other constants} = 0 \, .$$

$$\cdots\cdots\cdots\cdots(17)$$

Therefore, the stresses are obtained as follows:

$$\sigma_r = \frac{b^2}{b^2-a^2}(1-a^2r^{-2})p \, ,$$

$$\sigma_\theta = \frac{b^2}{b^2-a^2}(1+a^2r^{-2})p \, ,$$

$$\tau_{r\theta} = 0 \, .$$

$$\cdots\cdots\cdots\cdots(18a)$$

Especially, on the inner and outer surfaces,

$$(\sigma_\theta)_{r=a} = \frac{2b^2}{b^2-a^2}p,$$

$$(\sigma_\theta)_{r=b} = \frac{b^2+a^2}{b^2-a^2}p.$$

$$\left.\right\} \qquad \cdots\cdots\cdots\cdots(18b)$$

3. Discussion of the stress in a lining caused by earth pressure

In order to discuss the stress in a shaft lining caused by earth pressure, it is essential to know the distribution of the tangential stress on the inner and outer surfaces, because the greatest of the stresses on either surface is, at the same time, the maximum stress on the horizontal section. Therefore, the stress distribution on the inner and outer surfaces will be compared for various states of earth pressure, assuming that the total earth pressure is constant, to show how the stress is influenced by the state of the earth pressure. The stress distributions on the inner and outer surfaces of a lining, calculated by Eqs. (9)~(18b) for nine cases of earth pressure, shown in Fig. 9, assuming that $b/a=1.25$, are illustrated in Fig. 10, the tangential stress at each point on the inner and outer surfaces being plotted on a normal to the surface drawn from each point, depending on the scale shown at the foot of the figure. Tensile stresses are plotted on the normals directed toward the center of the lining, the compressive stresses on the normals drawn outwards from the surface. In any case, stresses are represented as multiples of the average earth pressure $\bar{p}$ in order to make it easy to compare the stresses under various states of earth pressure. The average earth pressure is defined as the total sum of earth pressure acting normal to the outer surface divided by the area of the outer surface, namely

for intermittent earth pressures:

$$\bar{p} = \frac{1}{2\pi}\int_0^{2\pi} p\,d\theta, \qquad\qquad \cdots\cdots\cdots\cdots(19a)$$

for a uniform earth pressure:

$$\bar{p} = p_0, \qquad\qquad \cdots\cdots\cdots\cdots(19b)$$

for an earth pressure distributed elliptically,

$$\bar{p} = \frac{1}{2\pi}\int_0^{2\pi} p\cos^2\theta\,d\theta = \frac{1}{2}p. \qquad\qquad \cdots\cdots\cdots\cdots(19c)$$

For the states of earth pressure shown in Fig. 9 (2) and (3), the maximum tensile stress $(\sigma_t)_{max}$ appears at the point on the inner surface where $\theta=0$ or $\theta=\pi$, whereas the maximum compressive stress $(\sigma_c)_{max}$ at the point on the inner
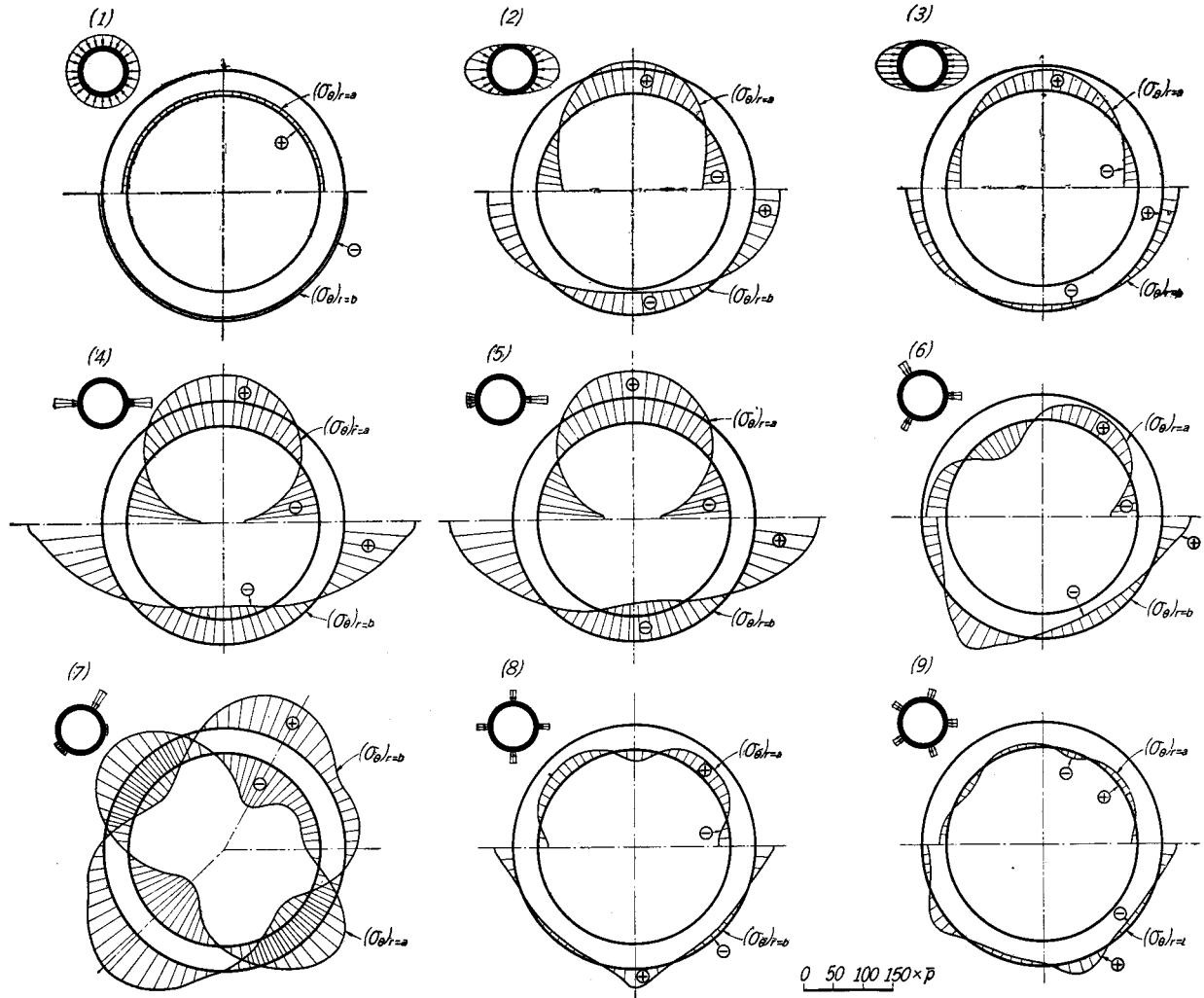
Fig. 10.   Results of analysis.   Plus signs indicate compressive stresses, while minus signs tensile stresses.

surface where $\theta = \dfrac{\pi}{2}$ or $\theta = \dfrac{3}{2}\pi$. For the states of earth pressure shown in Fig. 9 (4), (5), (6), (8) and (9), the maximum tensile stress $(\sigma_t)_{\max}$ appears at the intersection of the inner surface and the radius passing through the center of each distributed earth pressure, whereas the maximum compressive stress $(\sigma_c)_{\max}$ occurs at each center of the distributed earth pressure on the outer surface. In the case of a uniform earth pressure, there is no tensile stress, and the maximum compressive stress occurs uniformly along the inner surface.

In the case of a non-uniform earth pressure, of average value $\bar{p}$, it is evident from Fig. 10 that we obtain a far greater maximum compressive stress than one that appears under a uniform earth pressure p_0, if p_0 is equal to $\bar{p}$, and that the maximum tensile stress is nearly as great as the maximum compressive stress.

Prof. F. Mohr analysed the stress in a circular shaft lining subjected to an earth pressure such as shown in Fig. 9 (2) by the theory of the strength of materials[4]. His results are very close to ours but yield values somewhat lower.

It is supposed that the range of distribution of intermittent earth pressure may affect the stress arising in a lining, even though the total earth pressure is kept constant. To examine this point, the relation between the angle ϕ and the maximum tangential stresses, $(\sigma_t)_{\max}$ and $(\sigma_c)_{\max}$, is investigated and shown in Fig. 11, assuming that the earth pressure is distributed over two comparatively narrow ranges located diametrically opposite each other. From Fig. 11, it is seen that the maximum stress decreases with an increase in the range of earth pressure distribution, the total earth pressure being assumed constant, but this tendency is not great*.

Fig. 11. Relation between ϕ and $(\sigma_t)_{\max}$. or $(\sigma_c)_{\max}$.

The stress in a lining is influenced by the thickness of the lining. The relation between b/a and $(\sigma_t)_{\max}$ or $(\sigma_c)_{\max}$ is illustrated in Fig. 12 for five states of earth pressure. From this figure, it is noted that the maximum tensile or compressive stress increases rapidly as the lining become thinner, i.e. b/a decreases.

Assume that uniform earth pressures are distributed over a number of narrow ranges of an equal length at regular intervals on the outer surface. Let the
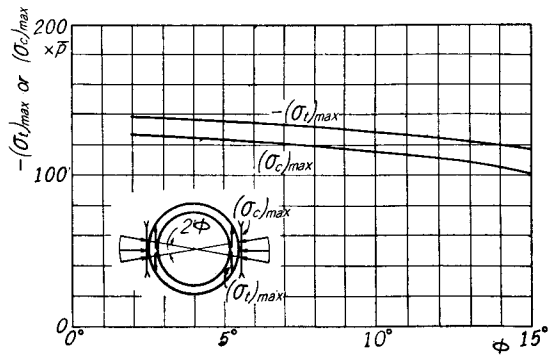
---

* Even when ϕ tends to zero, the tangential stress does not become very great. In such a case, however, the radial stress at the point where the earth pressure acts becomes very great.
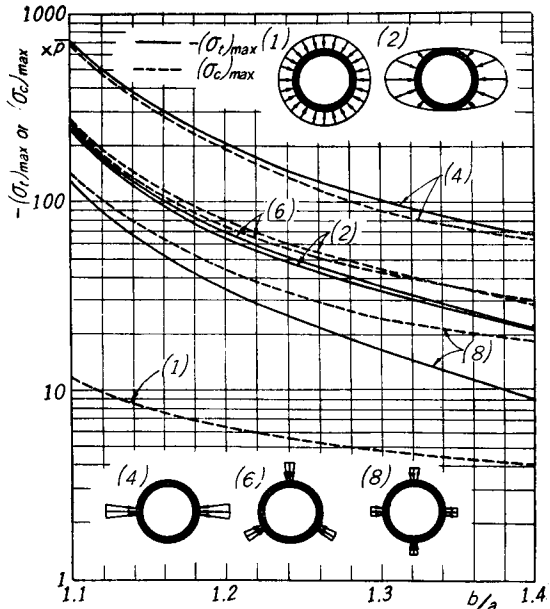
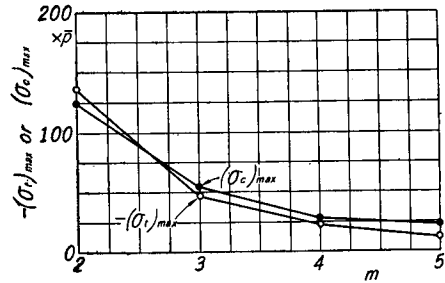Fig. 12. Relation between b/a and $(\sigma_t)_{max}$. or $(\sigma_c)_{max}$.

Fig. 13. Relation between m and $(\sigma_t)_{max}$. or $(\sigma_c)_{max}$.

number of the earth pressures be m. The relation between m and $(\sigma_t)_{max}$ or $(\sigma_c)_{max}$ is shown in Fig. 13. From this figure, it is seen that so long as the total earth pressure is kept constant, $(\sigma_t)_{max}$ or $(\sigma_c)_{max}$ is greatest when $m=2$, i.e. when the earth pressure acts on the lining at two diametrically opposite sections, and that $(\sigma_t)_{max}$ or $(\sigma_c)_{max}$ decreases with an increase in m. The maximum compressive stress $(\sigma_c)_{max}$ in the case where $m=2$ is 15~60 times the maximum compressive stress under a uniform earth pressure, according to the value of the ratio b/a, assuming that $p=\bar{p}_0$. In the case where the earth pressure is distributed elliptically, $(\sigma_t)_{max}$ and $(\sigma_c)_{max}$ are lower than in the case of $m=2$. Under an earth pressure such as shown in Fig. 9 (2), $(\sigma_t)_{max}$ is approximately one third the maximum tensile stress of the case where $m=2$, while $(\sigma_c)_{max}$ is approximately 1/2.5 times the maximum compressive stress of that case.

It is a matter of course that the stress caused by the combined earth pressures, uniform and irregular, is the algebraic sum of the stresses which are caused by the uniform and irregular earth pressure acting separately, according to the law of superposition.

It should be noted that all the results described above are correct so far as the concrete linings are perfectly elastic, but since concrete has imperfect elasticity, these results must be corrected. Roughly speaking the true maximum tensile stress may be about half the theoretical value mentioned above, whereas the true maximum compressive stress may be of about the same magnitude as the theoretical value, judging from the authors' investigation[5] published previously.

In the design of a shaft lining, one of problems is to estimate the possible maximum stress in the lining. The following is the author's proposal for this estimation, assuming that the uniform and irregular earth pressures, p_0 and $\bar{p}$, can be estimated to some extent by considering the condition of the ground and by consulting actual data of stress measurement.

So long as $\bar{p}$ is kept constant, the worst state of stress in a lining occurs when the irregular earth pressure consists of two concentrated pressures acting diametrically opposite to each other, but the state of stress is much improved when it is distributed in such a manner as an ellipse.

First calculate the maximum tensile and compressive stresses assuming that the irregular earth pressure is concentrated over two narrow ranges located diametrically opposite to each other, and make them the upper limits of the tensile and compressive stresses due to the irregular earth pressure. Second, calculate the maximum tensile and compressive stresses assuming that the irregular earth pressure is distributed elliptically, and make then the lower limits of the tensile and compressive stresses due to the irregular earth pressure. In addition, the compressive stress caused by the uniform earth pressure must be taken into account. Then, considering the nature of the ground into which a shaft is sunk, properly estimate the possible maximum tensile and compressive stresses between the upper and lower limits of stress.

To calculate rapidly the upper limits of the tensile and compressive stresses, $(\sigma_t)_U$ and $(\sigma_c)_U$, and the lower limits, $(\sigma_t)_L$ and $(\sigma_c)_L$, the authors wish to propose the following approximate formulas.

$$\left.\begin{aligned}
(\sigma_t)_U &\fallingdotseq \frac{2b^2}{b^2-a^2}p_0 - 3\left\{\frac{2b^2(b^2+3a^2)}{(b^2-a^2)^2}\right\}\bar{p}, \\
(\sigma_c)_U &\fallingdotseq \frac{b^2+a^2}{b^2-a^2}p_0 + 2.5\left\{\frac{2b^2(3b^2+a^2)}{(b^2-a^2)^2}\right\}\bar{p}, \\
(\sigma_t)_L &= \frac{2b^2}{b^2-a^2}p_0 - \frac{2b^2(b^2+3a^2)}{(b^2-a^2)^2}\bar{p}, \\
(\sigma_c)_L &= \frac{2b^2}{b^2-a^2}p_0 + \frac{2b^2(3b^2+a^2)}{(b^2-a^2)^2}\bar{p}.
\end{aligned}\right\} \quad \cdots\cdots\cdots\cdots(20)$$

Ex. 1 When the earth pressure acting on a shaft lining is as shown in Fig. 14*, we obtain:

$$p_0 = 0.08 \text{ kg/cm}^2 ,$$

total irregular earth pressure $= 79600 \text{ kg/cm}$
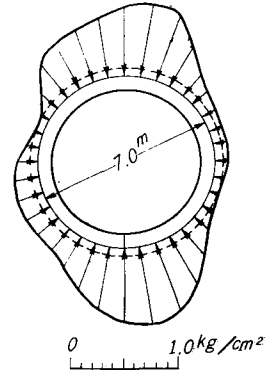
$$\bar{p} = 0.36 \text{ kg/cm}^2 .$$

Fig. 14. An example of earth pressure distribution.

* Cited from Reference (1). The tubbing of this shaft was destroyed by earth pressure.

From these data, the upper and lower limits of the possible maximum stresses are estimated according to Eq. (20) as shown in Table 3.

Table 3. Estimation of the upper and lower limits of maximum tensile and compressive stresses, referring to Example 1.

b/a	1.1		1.2		1.3	
Maximum stress	tensile (kg/cm^2)	compressive (kg/cm^2)	tensile (kg/cm^2)	compressive (kg/cm^2)	tensile (kg/cm^2)	compressive (kg/cm^2)
Upper limit	250	250	84	84	30	34
Lower limit	83	93	28	34	10	14

Ex. 2 When the earth pressure acting on a shaft lining is estimated as:

$$p_0 = 10 \, kg/cm^2 ,$$

$$\bar{p}/p_0 = 0.05 \quad ,$$

the upper and lower limits of the possible maximum stresses are calculated in the same manner as in Ex. 1, as shown in Table 4.

Table 4. Estimation of the upper and lower limits of maximum tensile and compressive stresses, referring to Example 2.

b/a	1.1		1.2		1.3	
Maximum stress	tensile (kg/cm^2)	compressive (kg/cm^2)	tensile (kg/cm^2)	compressive (kg/cm^2)	tensile (kg/cm^2)	compressive (kg/cm^2)
Upper limit	226	432	51	160	8	90
Lower limit	0.3	242	—	112	—	59

4. Conclusion

In Part II the results of analytical studies on the stress in a circular shaft lining caused by the earth pressure distributed uniformly or irregularly were described. By employing the results obtained, the stress distributions on the inner and outer surfaces of a shaft lining subjected to nine states of earth pressure were calculated.

If the total earth pressure remains constant, the maximum stress appearing in a lining is much affected by the distribution of the earth pressure. Namely, when concentrated earth pressures act on a lining at diametrically opposite sections, the maximum compressive stress amounts to 15~60 times that under a uniform earth pressure, and the maximum tensile stress is of the same magnitude as the maximum compressive stress. When the earth pressure is distributed elliptically, the maximum compressive and tensile stresses are about 1/2.5 and 1/3

times those which appear under two concentrated earth pressures acting diametrically opposite to each other.

As the area on which the concentrated earth pressures are distributed or the thickness of the lining increases, the maximum compressive and tensile stresses decrease.

As the number of the concentrated earth pressures increases, the maximum stresses also decrease.

The authors have presented a method for estimating the possible maximum tensile and compressive stresses in a shaft lining that should be taken into account in designing a shaft lining.

References

1) B. Bals: Glückauf, **85**, 367 (1949).
   F. Mohr: Glückauf, **86**, 437 (1950).
   F. Wansleben: Glückauf, **89**, 1129 (1953).
   A. Крупенников: Шахтное Строительство 12 (1959-1).
   R. Shepherd, A. H. Wilson: Coll. Guard., **200**, 285 (1960).
2) Y. Hiramatsu, Y. Niwa, Y. Oka: Technical Reports of the Engineering Research Institute Kyoto University VII 3, Report No. 37 (1957).
   Y. Hiramatsu, Y. Niwa, Y. Oka: Suiyo Kai-shi, **14** 7 (1959).
3) Y. Hiramatsu, Y. Oka: Journ. Min. Met. Inst. Japan, **68**, 545 (1952).
4) F. Mohr: loc. cit.
5) Y. Hiramatsu, Y. Oka: THIS MEMOIRS **21**, 128 (1959).